BMC Biology

RESEARCH ARTICLE

Open Access

Diminished activation of excitatory neurons in the prelimbic cortex leads to impaired working memory capacity in mice

Li-Xin Jiang[1,2,3†], Geng-Di Huang[4,5†], Yong-Lu Tian[6,7], Ri-Xu Cong[8], Xue Meng[9], Hua-Li Wang[1,2,3*], Chen Zhang[10*] and Xin Yu[1,2,3*]

Abstract

Background Working memory capacity impairment is an early sign of Alzheimer's disease, but the underlying mechanisms remain unclear. Clarifying how working memory capacity is affected will help us better understand the pathological mechanism of Alzheimer's disease. We used the olfactory working memory capacity paradigm to evaluate memory capacity in 3-month-old 5XFAD (an animal model of Alzheimer's disease) mice. Immunofluorescence staining of the prefrontal cortex was performed to detect the number of FOS-positive neurons, calmodulin-dependent protein kinase II-positive neurons, and glutamate decarboxylase-positive neurons in the prelimbic cortex and infralimbic cortex. A chemogenetic method was then used to modulate the inhibition and activation of excitatory neurons in the prelimbic cortex of wild-type and 5XFAD mice and to measure the memory capacity of mice.

Results Working memory capacity was significantly diminished in 5XFAD mice compared to littermate wild-type mice. Neuronal activation of the prelimbic cortex, but not the infralimbic cortex, was attenuated in 5XFAD mice performing the olfactory working memory capacity task. Subsequently, the FOS-positive neurons were co-localized with both calmodulin-dependent protein kinase II-positive neurons and glutamate decarboxylase-positive neurons. The results showed that the activation of excitatory neurons in the prelimbic cortex was correlated with working memory capacity in mice. Our results further demonstrate that the chemogenetic inhibition of prelimbic cortex excitatory neurons resulted in reduced working memory capacity in wild-type mice, while the chemogenetic activation of prelimbic cortex excitatory neurons improved the working memory capacity of 5XFAD mice.

Conclusion The diminished activation of prelimbic cortex excitatory neurons in 5XFAD mice during task performance is associated with reduced working memory capacity, and activation modulation of excitatory neurons by chemogenetic methods can improve memory capacity impairment in 5XFAD mice. These findings may provide a new direction for exploring Alzheimer's disease therapeutic approaches.

Keywords Alzheimer's disease, Working memory capacity, 5XFAD mice, FOS, Excitatory neuron

†Li-Xin Jiang and Geng-Di Huang contributed equally to this work.

*Correspondence:
Hua-Li Wang
huali_wang@bjmu.edu.cn
Chen Zhang
czhang@ccmu.edu.cn
Xin Yu
yuxin@bjmu.edu.cn
Full list of author information is available at the end of the article

Introduction

Alzheimer's disease (AD) is an age-dependent neurodegenerative brain disease that is the leading cause of dementia in the elderly population [1, 2]. The neuropathology of AD is characterized by extracellular Aβ plaques and intraneuronal neurofibrillary tangles accompanied by neuronal dysfunction/death and synapse loss [3–5]. The main clinical symptoms of AD are progressive memory loss and cognitive deterioration [6, 7]. As the disease progresses, AD patients gradually develop impairments in episodic memory, semantic memory, working memory (WM), and visuospatial memory [8–11]. Of these, impairment of WM is evident as early as in mild cognitive impairment, also referred to as the preclinical stage of AD, and worsens with progression to AD [12, 13]. Furthermore, WM deficits are central in normal neurocognitive aging and the rapid cognitive deterioration associated with dementias, such as AD [14, 15]. WM deficits in AD are thought to be responsible for several significant problems, such as difficulty dividing attention and manipulating remembered information [16, 17]. Compared to healthy controls, AD patients are more likely to be overloaded with information and exhibit rapid performance decline as task demands increase [18]. Therefore, it is of great interest to determine the mechanisms of WM impairment, which may provide a new direction for therapeutic approaches to AD.

WM is a vital process of the brain that actively maintains and processes information during a delay of a few seconds after sensory input is received and before behavior begins [19–22]. It is thought to be the core cognitive process that supports a range of behaviors, from perception to problem-solving and action control [23]. Working memory capacity (WMC) is a crucial component of WM and is the ability to retain information for a few seconds [19]. It is limited, and a restricted amount of information or number of items is actively retained in WM [24, 25]. Clarifying the mechanisms underlying the formation of WMC would facilitate the interpretation of the impairment of memory capacity in AD patients. Exploratory studies of WM mechanisms have focused more on the brain regions involved in WM and the electrical activity of neurons. The study of brain regions related to WM has shown that multiple regions of the brain are involved, and a great deal of research has shown that the prefrontal cortex (PFC) is critical for WM [26–28]. Disturbances to PFC activity during delays in the dorsolateral PFC in primates and medial PFC (mPFC) neurons in rodents impaired WM and WM-related activity [29–33]. Moreover, during behavior, neurons in the PFC exhibit highly diverse responses [34, 35].

In recent years, there has been increasing interest in how WM is affected in the early stages of AD. In our previous study, we developed a novel olfactory working memory capacity (OWMC) paradigm [36, 37] inspired by the rodent odor span task established by Dudchenko et al. [38] and Young et al. [39]. In this paradigm, we introduced a method for measuring the WMC of trial-specific information that we can use to assess the performance of mice from low to high loads of memory information. In this study, we will assess the impairment of WMC in 3-month-old 5XFAD (TG) mice using the OWMC paradigm. Previously, we found that 5XFAD mice have diminished neuronal activation in the mPFC while performing a task. We wanted to explore which subregions (prelimbic cortex [PrL] and infralimbic cortex [IL]) of the mPFC differ in neuronal activation during task performance. After specifying the brain regions associated with the OWMC task, we will go further to determine which type of neurons (excitatory and inhibitory) are involved in performing the task. Finally, we will apply a chemogenetic method to modulate the inhibition and activation of specific neurons in wild-type (WT) and 5XFAD mice to determine whether we can reduce WMC in WT mice and ameliorate WMC impairment in 5XFAD mice.

Results

WMC was significantly reduced in 3-month-old 5XFAD mice

At the beginning of this study, we used the OWMC paradigm to assess the WMC of 3-month-old 5XFAD mice. During the nonmatching to a single odor sample (NMSS) rule-learning phase, we recorded the responses of mice for each trial and counted the performance accuracy (Fig. 1a), correct selection rate (Fig. 1b), and correct rejection rate (Fig. 1c). There was no difference between WT and 5XFAD mice in these indices (all $p > 0.05$). Next, for 4 days of nonmatching to multiple odor samples (NMMS) rule-learning, we measured the daily memory capacity of mice and found that WT and 5XFAD mice showed similar WMC ($p > 0.05$, Fig. 1d). It was clear that both 5XFAD and WT mice could learn the NMSS and NMMS rules well. Finally, the capacity test was performed for 3 days. We recorded the WMC of each mouse (Fig. 1e). We counted the accuracy of mice with different memory capacities (Fig. 1f) as well as the average number of errors (Fig. 1h), and we calculated the percentage of mice that could complete different memory capacity tasks (Fig. 1g). We found that the WMC was significantly diminished in 5XFAD mice (Day-1: $t = 3.96$, $p < 0.001$; Day-2: $t = 4.22$, $p < 0.001$; Day-3: $t = 4.18$, $p < 0.001$) compared to littermate WT mice. As the memory load increased, 5XFAD mice made significantly more errors than WT mice ($F_{(1, 819)} = 18.13$, $p < 0.0001$) and had a significantly lower accuracy ($F_{(1, 1254)} = 84.52$, $p < 0.0001$).

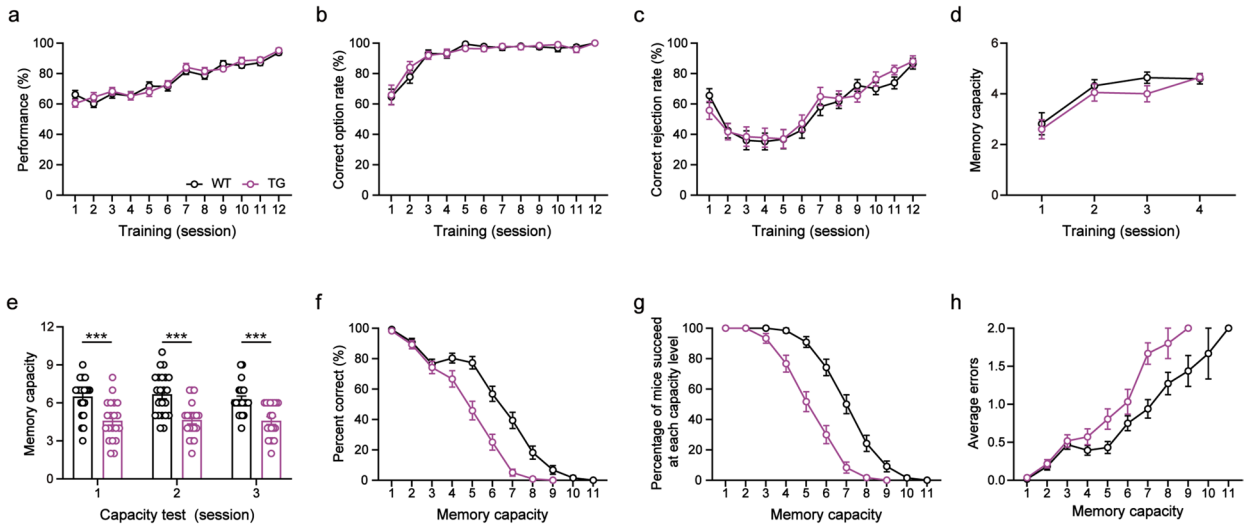

Fig. 1 WMC was significantly reduced in 3-month-old 5XFAD mice compared to littermate WT mice. **a-c** Performance correct rate, correct option rate and correct rejection rate of mice during the NMSS-rule learning phase (Two-way ANOVA, all $p > 0.05$). **d** WMC of mice during the NMMS-rule learning phase (Two-way ANOVA, $p > 0.05$). **e** WMC of mice during the test phase (Unpaired Student's *t* test, ***$p < 0.001$). **f** Percent correct at each capacity level (Two-way ANOVA, ****$p < 0.0001$). **g** Percentage of mice succeeded at each capacity level (Two-way ANOVA, ****$p < 0.0001$). **h** Average errors at each capacity level (Two-way ANOVA, ****$p < 0.0001$). WT: $n = 22$; TG: $n = 20$. Data are presented as the mean ± SEM

Additionally, 5XFAD mice completed the task at a significantly lower percentage than WT mice ($F_{(1, 1254)} = 137.10$, $p < 0.0001$). Therefore, we conclude that the WMC of 3-month-old 5XFAD mice is significantly lower than that of WT mice.

Neuronal activation of the PrL was attenuated in 5XFAD mice performing the OWMC task

In a previous study [36], we found that neuronal activation of the mPFC was attenuated in 5XFAD mice while performing a task. We wanted to explore which subregions of the mPFC (the PrL, IL, or both; Fig. 2c) have activation differences in neurons while performing the task. The mice were divided into 4 groups: WT + no OWMC task, 5XFAD + no OWMC task, WT + OWMC task, and 5XFAD + OWMC task. We calculated the number of FOS-positive (FOS^+) neurons in the two brain regions (Fig. 2a, b). We then found that the number of FOS^+ neurons in the PrL were significantly higher in the task group mice than in the nontask group mice (task: $F_{(1, 44)} = 32.19$, $p < 0.0001$; Fig. 2d), but not in the IL (task: $F_{(1, 44)} = 2.19$, $p > 0.05$; Fig. 2f). In the task group, the number of FOS^+ neurons in the PrL were significantly lower in 5XFAD mice than in WT mice (genotype: $F_{(1, 44)} = 4.50$, $p < 0.05$; Task-TG vs. Task-WT: $p < 0.05$, Tukey's tests; Fig. 2d). We also conducted a correlation analysis between the number of FOS^+ neurons and the WMC of task group mice. We found a positive correlation between the number of FOS^+ neurons in the PrL and WMC ($r = 0.81$, $p < 0.05$; Fig. 2e), while there was no correlation between the number of FOS + neurons in the IL and WMC ($r = 0.26$, $p > 0.05$; Fig. 2g). These results indicate that 5XFAD mice exhibit diminished neuronal activation of the PrL when performing the OWMC task.

Activation of excitatory neurons was associated with WMC

Different types of neurons in the mPFC play different roles in encoding and regulating behaviors [40]. To investigate which specific types of neurons are associated with WMC, we performed double immunostaining against FOS and the marker of excitatory neurons (CaMKII, Fig. 3a) or inhibitory neurons (GAD, Fig. 3b). We found that the number of FOS^+ neurons co-localized with calmodulin-dependent protein kinase II-positive ($CaMKII^+$) neurons was significantly higher in the task group of WT mice than in the task group of 5XFAD mice (genotype: $F_{(1, 50)} = 5.88$, $p < 0.05$; Task-TG vs. Task-WT: $p < 0.05$, Tukey's tests; Fig. 3c). Furthermore, a linear relationship was observed between the number of FOS^+ neurons and the number of FOS^+ neurons co-localized with $CaMKII^+$ neurons ($r = 0.96$, $p < 0.0001$; Fig. 3d). As the number of FOS^+ neurons increased, there was a concomitant increase in the number of FOS^+ neurons that co-localized with $CaMKII^+$ neurons. However, we did not detect a difference in the number of FOS^+ neurons co-localized with glutamate decarboxylase-positive (GAD^+) neurons between the four groups (task: $F_{(1, 32)} = 0.01$, $p > 0.05$; genotype: $F_{(1, 32)} = 0.01$, $p > 0.05$; Fig. 3e). Thus, we suggest that WMC is associated with the activation of excitatory neurons in the PrL.

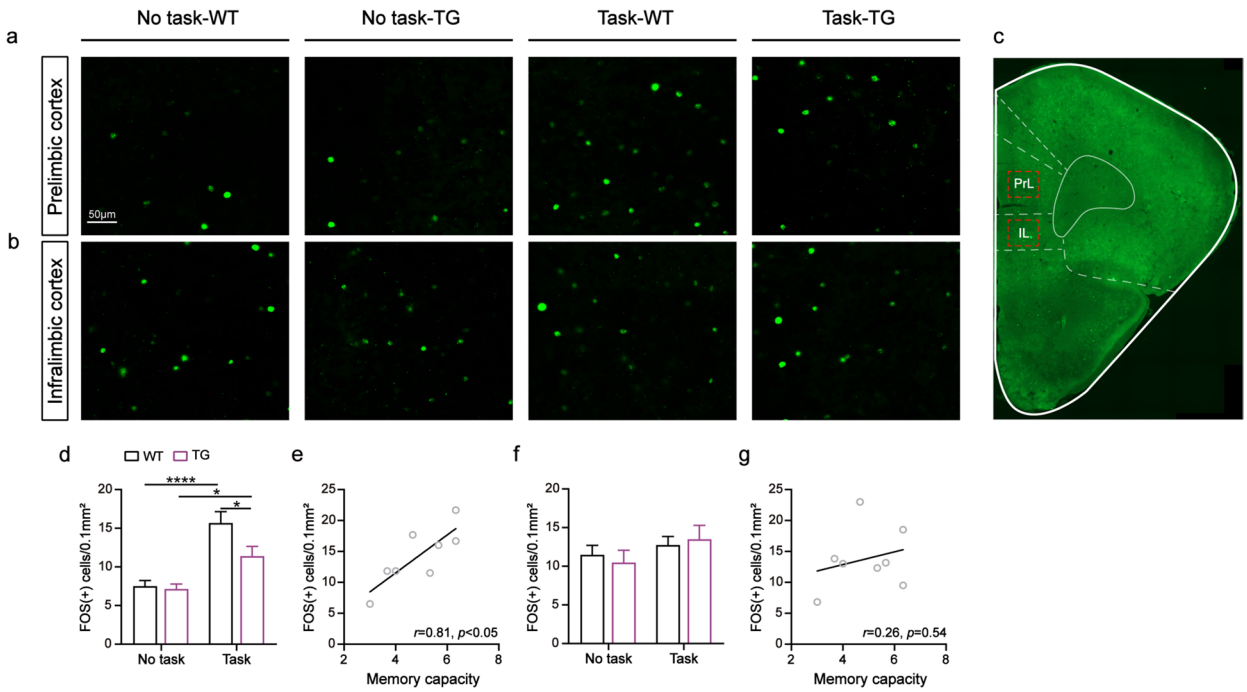

Fig. 2 The activation of PrL neurons was associated with WMC. **a,b** Representative images show the FOS$^+$ neurons in the PrL and IL of each group of mice. **c** Representative image show the PrL and IL. **d** The number of FOS$^+$ neurons in the PrL (Two-way ANOVA, interaction: $p > 0.05$, task: $p < 0.0001$, genotype: $p < 0.05$; post hoc Tukey's tests, *$p < 0.05$, ****$p < 0.0001$). $n = 12$ slices from four mice per group. **e** Relationship between the number of FOS$^+$ neurons in the PrL and WMC in the task group mice (Linear regression, *$p < 0.05$). $n = 8$. **f** The number of FOS$^+$ neurons in the IL (Two-way ANOVA, all $p > 0.05$; post hoc Tukey's tests, all $p > 0.05$). $n = 12$ slices from four mice per group. **g** Relationship between the number of FOS$^+$ neurons in the IL and WMC of in the task group mice (Linear regression, $p > 0.05$). $n = 8$. Data are presented as the mean ± SEM

Chemogenetic inhibition of PrL excitatory neurons attenuated the WMC of WT mice

To further test whether PrL excitatory neurons are associated with WMC, the DREADD (designer receptors exclusively activated by designer drugs)-based tools were used. We bilaterally injected the inhibitory virus (hM4Di-mCherry) or non-functional control virus (mCherry) into the PrL of WT mice (Fig. 4a). To ensure that the virus (hM4Di-mCherry) was effective, whole-cell recordings were performed in PrL neurons (Fig. 4d). The administration of Clozapine-N-oxide (CNO) inhibited the activity of PrL neurons expressing hM4Di, which led to an increase in the minimum required injection current for the induction of action potentials ($t = 4.37$, $p < 0.01$; Fig. 4b) and a reduction in the number of spikes ($F_{(1,\ 207)} = 82.60$, $p < 0.0001$; Fig. 4c). To establish a baseline before administering CNO (saline injection), we conducted a three-day capacity test on mice injected with hM4Di. Subsequently, we administered CNO to both hM4Di-injected and mCherry-injected mice and evaluated their WMC. Compared to mice injected with mCherry, we observed a significant decrease in WMC in mice injected with hM4Di ($t = 4.04$, $p < 0.01$; Fig. 4e). As the memory load increased, the percent correct in the hM4Di injection group was significantly lower than that of the control group (injected with mCherry, $F_{(1,\ 328)} = 39.89$, $p < 0.0001$; Fig. 4f), and the percentage of task completion was also lower ($F_{(1,\ 328)} = 44.19$, $p < 0.0001$; Fig. 4g). Similarly, we found that the WT mice with inhibited excitatory neuronal activity in the PrL showed a significant decrease in memory capacity ($t = 3.92$, $p < 0.01$; Fig. 5h) compared to their baseline. As the memory load increased, the percent correct decreased significantly after excitatory neuronal activity was inhibited ($F_{(1,\ 388)} = 57.99$, $p < 0.0001$; Fig. 4i). Additionally, they completed the task at a significantly lower percentage than before ($F_{(1,\ 388)} = 64.37$, $p < 0.0001$; Fig. 4j). These results suggest that inhibiting the activity of PrL excitatory neurons can attenuate the WMC in WT mice.

Chemogenetic activation of PrL excitatory neurons improved the WMC of 5XFAD mice

We hypothesized that if the inhibition of PrL excitatory neuronal activity is responsible for reduced WMC, then activating these neurons may ameliorate WMC impairment in 5XFAD mice. To test our hypothesis, we

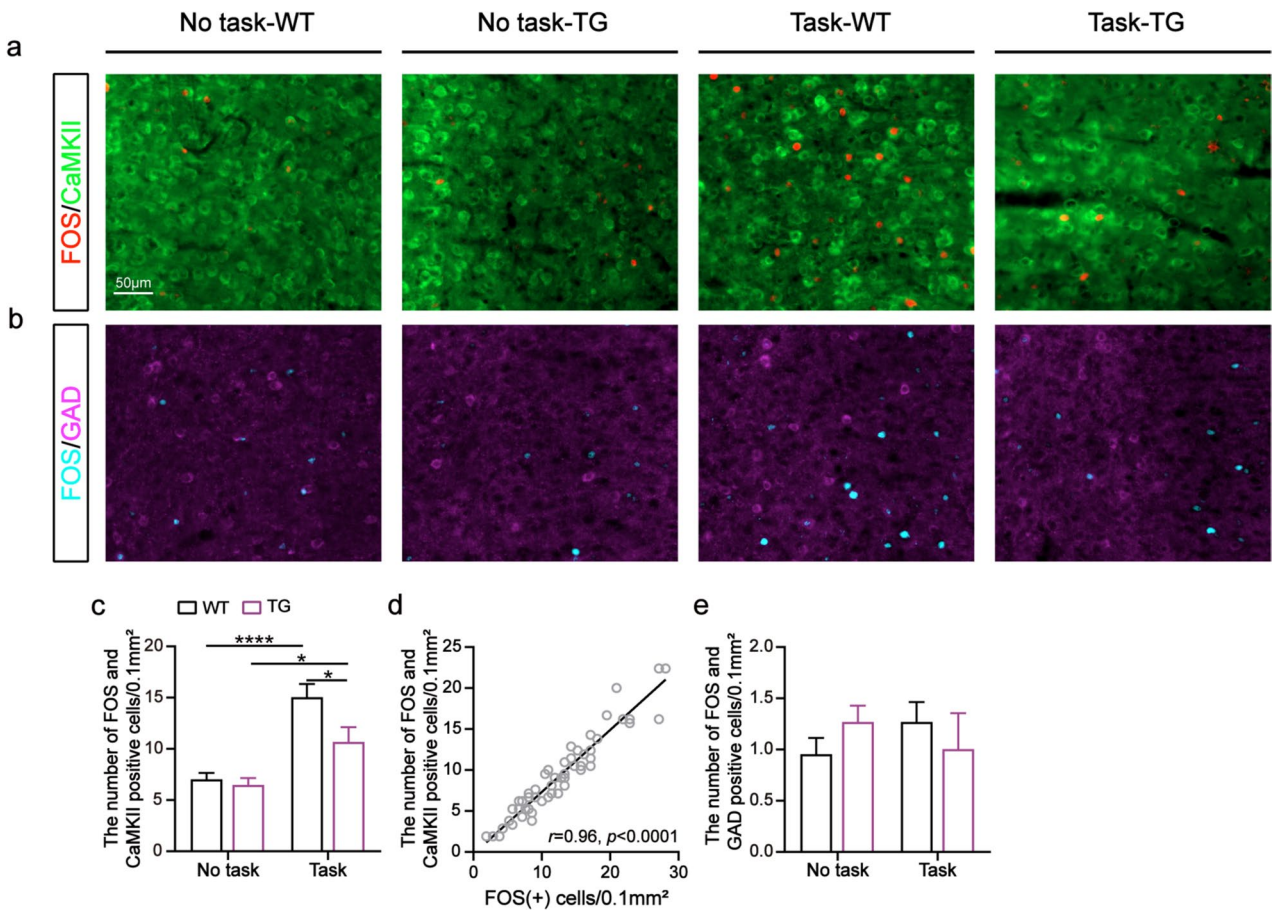

Fig. 3 The activation of excitatory neurons was associated with WMC. **a** Representative images showing the FOS$^+$ neurons, CaMKII$^+$ neurons and co-localized cells in the PrL of each group of mice. **b** Representative images showing the FOS$^+$ neurons, GAD$^+$ neurons and co-localized cells in the PrL of each group of mice. **c** The number of FOS$^+$ neurons co-localized with CaMKII$^+$ neurons (Two-way ANOVA, interaction: $p > 0.05$, task: $p < 0.0001$, genotype: $p < 0.05$; post hoc Tukey's tests, $^*p < 0.05$, $^{****}p < 0.0001$). No task: $n = 15$ slices from five mice per group; Task: $n = 12$ slices from four mice per group. **d** Relationship between the amount of FOS$^+$ neurons and FOS$^+$ neurons co-localized with CaMKII$^+$ neurons (Linear regression, $^{****}p < 0.0001$). $n = 54$ slices from eighteen mice. **e** The number of FOS$^+$ neurons co-localized with GAD$^+$ neurons (Two-way ANOVA, all $p > 0.05$; post hoc Tukey's tests, all $p > 0.05$). $n = 9$ slices from three mice per group. Data are presented as the mean ± SEM

bilaterally injected excitatory virus (hM3Dq-mCherry) or mCherry encoding virus into the PrL of 5XFAD mice (Fig. 5a). As with WT mice, the effectiveness of the virus (hM3Dq-mCherry) was also verified by electrophysiological recordings (Fig. 5d). CNO administration activated the activity of hM3Dq-expressing PrL neurons, resulting in an increase in the number of spikes ($F_{(1,\ 239)} = 10.80$, $p < 0.01$; Fig. 5c) and a relative decrease in the minimum injection current required to induce action potentials ($t = 1.70$, $p = 0.13$; Fig. 5b). Initially, we examined the WMC of 5XFAD mice under natural conditions (saline injection) for three days. Next, we injected CNO into the 5XFAD mice with hM3Dq injection or mCherry injection and tested their WMC. Compared to the mCherry injection group, the hM3Dq injection group of 5XFAD mice exhibited a higher WMC ($t = 2.82$, $p < 0.05$; Fig. 5e). Additionally, as the memory load increased, the 5XFAD mice injected with hM3Dq showed higher rates of accuracy ($F_{(1,\ 321)} = 65.91$, $p < 0.0001$; Fig. 5f) and task completion ($F_{(1,\ 321)} = 51.11$, $p < 0.0001$; Fig. 5g). Furthermore, our findings showed that activating excitatory neuronal activity in the PrL led to significantly improved memory capacity in 5XFAD mice compared to baseline ($t = 3.97$, $p < 0.05$; Fig. 5h). As the memory load increased, their percent correct increased significantly ($F_{(1,\ 348)} = 41.42$, $p < 0.0001$; Fig. 5i) after excitatory neuronal activity was activated, and they completed the task at a higher percentage than before ($F_{(1,\ 348)} = 28.76$, $p < 0.0001$; Fig. 5j). Therefore, our results suggest that activating excitatory neurons in the PrL can ameliorate the WMC deficits in 5XFAD mice.

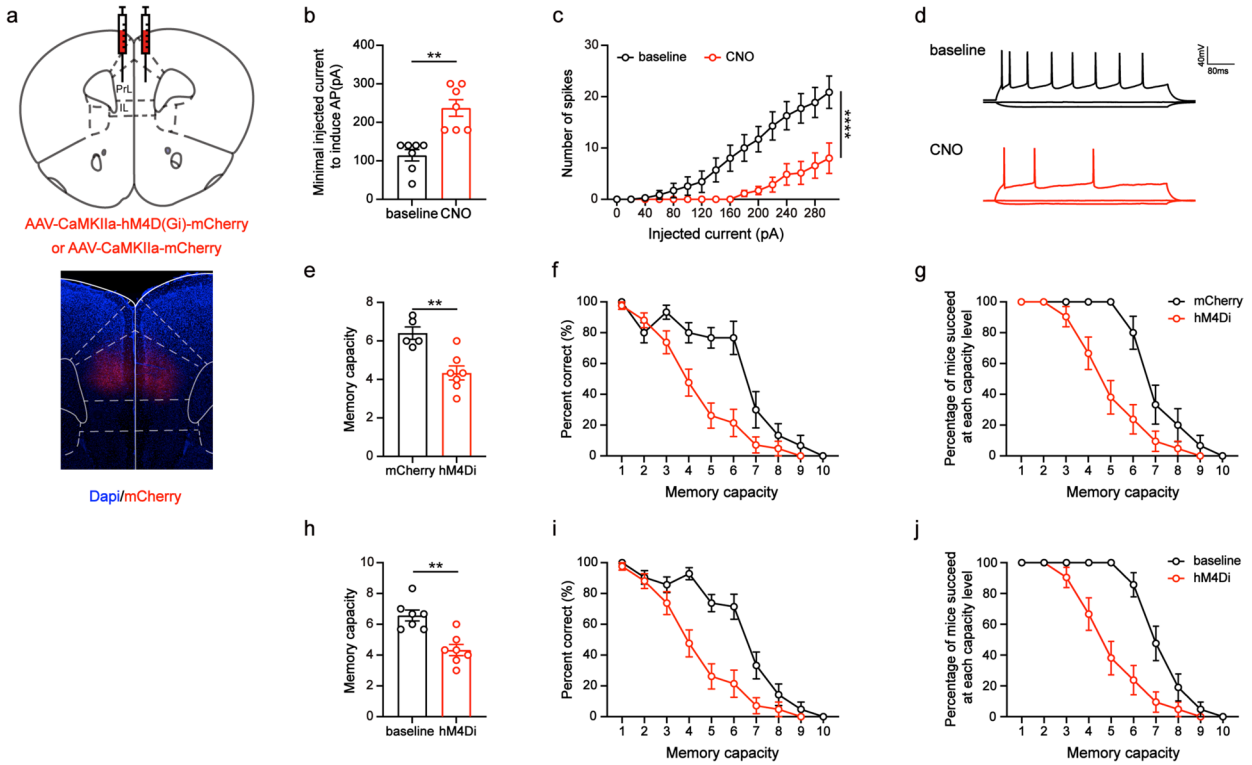

Fig. 4 Chemogenetic inhibition of PrL excitatory neurons attenuated the WMC of WT mice. **a** Schematic diagram (coronal section) showing the injection target of the virus (hM4Di-mCherry or mCherry) in the PrL. **B** The minimal injected current to induce action potential (Paired Student's *t* test, $^{**}p < 0.01$). $n = 7$. **c** The number of induced action potentials at different current steps (Two-way ANOVA, $^{****}p < 0.0001$). **d** Current–voltage relationship of a representative PrL neuron recorded before and during CNO perfusion. **e** The WMC of mice in the mCherry and hM4Di group (Unpaired Student's *t* test, $^{**}p < 0.01$). mCherry: $n = 5$; hM4Di: $n = 7$. **f** Percent correct at each capacity level of mice in the mCherry and hM4Di group (Two-way ANOVA, $^{****}p < 0.0001$). **g** Percentage of mice succeeded at each capacity level in the mCherry and hM4Di group (Two-way ANOVA, $^{****}p < 0.0001$). **h** The WMC of mice in the test phase before and during CNO perfusion (Paired Student's *t* test, $^{**}p < 0.01$). $n = 7$. **i** Percent correct at each capacity level of mice before and during CNO perfusion (Two-way ANOVA, $^{****}p < 0.0001$). **j** Percentage of mice succeeded at each capacity level before and during CNO perfusion (Two-way ANOVA, $^{****}p < 0.0001$). Data are presented as the mean ± SEM

Discussion

In recent years, the neurobiological mechanisms behind WM have received increasing attention. For different disorders, such as schizophrenia, AD, and attention deficit and hyperactivity disorder, the mechanisms of WM impairment may differ. Memory capacity is an essential component of WM. However, the neurobiological mechanisms behind WMC have yet to be well explored due to the lack of appropriate and effective behavioral paradigms for animals. Our previous work established a more sensitive and robust paradigm (the OWMC paradigm) for measuring WMC. In the present study, we used this paradigm to assess memory capacity impairment in 3-month-old 5XFAD mice and found that the WMC of 5XFAD mice was significantly lower than that of WT mice. By exploring the mechanisms responsible for this impairment, we found that the impairment of memory capacity in 5XFAD mice was associated with diminished activation of excitatory neurons in the PrL. To further demonstrate that attenuated activation of excitatory neurons in the PrL is associated with reduced WMC, we intervened by a chemogenetic method. We found that inhibition of excitatory neurons in the PrL impaired WMC in WT mice, whereas activation of excitatory neurons in the PrL ameliorated WMC impairment in 5XFAD mice.

5XFAD mice, which are widely used, recapitulate many AD-related phenotypes and have a relatively early and aggressive presentation. The mice accumulate high levels of intraneuronal $A\beta_{42}$ at approximately 1.5 months of age, and extracellular amyloid deposition begins at approximately 2 months [41]. 5XFAD mice show neuropathological changes very early, while cognitive impairment appears much later. The impairment of recognition memory and spatial reference memory in 5XFAD mice generally appears at 4–5 months of age [41–44]. In this study, we detected a significant decrease in the WMC of 3-month-old 5XFAD mice using the OWMC task. Thus,

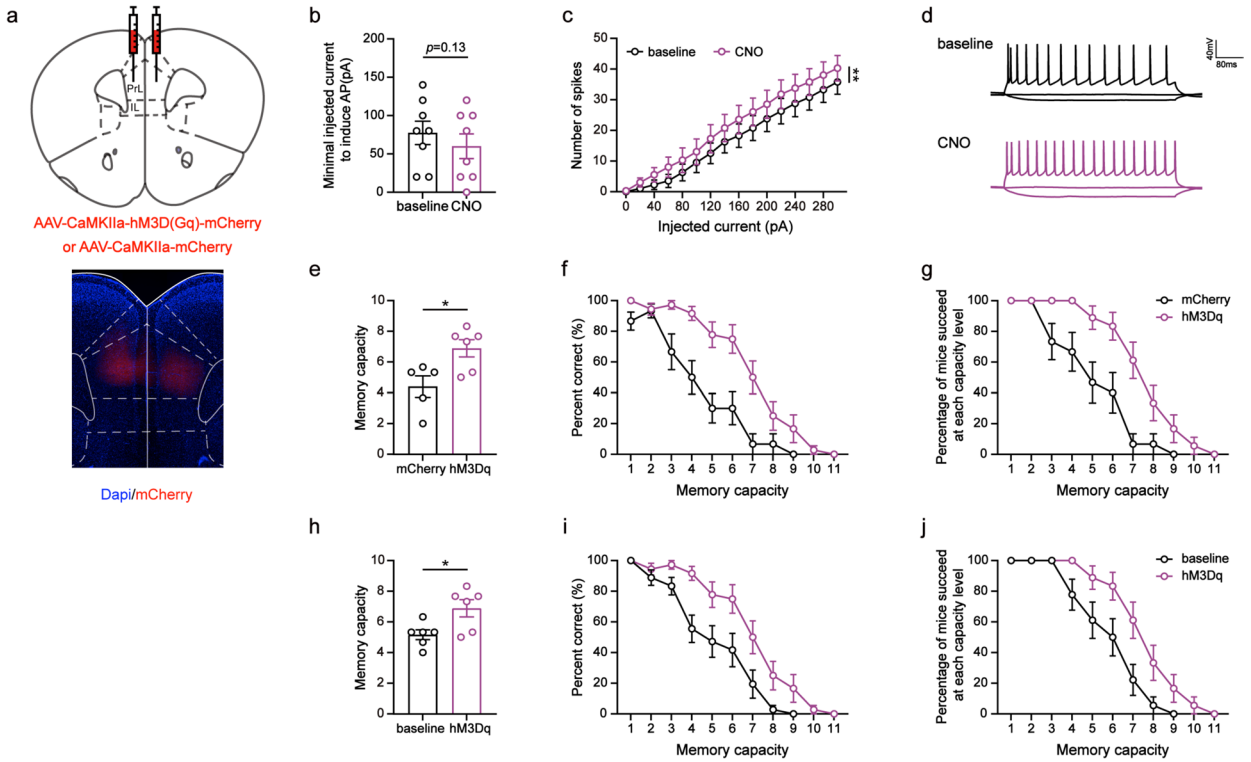

Fig. 5 Chemogenetic activation of PrL excitatory neurons improved the WMC of 5XFAD mice. **a** Schematic diagram (coronal section) showing the injection target of the virus (hM3Dq-mCherry or mCherry) in the PrL. **B** The minimal injected current to induce action potential (Paired Student's *t* test, $p = 0.13$). $n = 8$. **c** The number of induced action potentials at different current steps (Two-way ANOVA, $^{**}p < 0.01$). **d** Current–voltage relationship of a representative PrL neuron recorded before and during CNO perfusion. **e** The WMC of mice in the mCherry and hM3Dq group (Unpaired Student's *t* test, $^{*}p < 0.05$). mCherry: $n = 5$; hM3Dq: $n = 6$. **f** Percent correct at each capacity level of mice in the mCherry and hM3Dq group (Two-way ANOVA, $^{****}p < 0.0001$). **g** Percentage of mice succeeded at each capacity level in the mCherry and hM3Dq group (Two-way ANOVA, $^{****}p < 0.0001$). **h** The WMC of mice in the test phase before and during CNO perfusion (Paired Student's *t* test, $^{*}p < 0.05$). $n = 6$. **i** Percent correct at each capacity level of mice before and during CNO perfusion (Two-way ANOVA, $^{****}p < 0.0001$). **j** Percentage of mice succeeded at each capacity level before and during CNO perfusion (Two-way ANOVA, $^{****}p < 0.0001$). Data are presented as the mean ± SEM

we demonstrated that the OWMC paradigm has higher sensitivity than the common behavioral paradigm (i.e., novel object recognition test, Y-maze, and Morris water maze) for assessing cognitive function. This paradigm is more complex than the common behavioral paradigm. We trained mice over a long period to better learn the rules of the task. In the OWMC task, the sample odor for each trial is independent of the previous trial. The mice need to maintain increasing information from the list of odors and also use this information flexibly to make appropriate responses. During the testing phase, this paradigm can continuously increase the task's difficulty until the experimental animal fails to complete it. Thus, this paradigm can be more sensitive to detect changes in cognitive function.

We detected impairment of WMC in 5XFAD mice at an earlier age (3 months) through the OWMC paradigm. This led us to explore the neurobiological mechanisms involved. We first focused on the brain regions involved in WMC. In previous studies, several brain regions have been reported to be associated with the storage of WM information (i.e., the PFC [19, 45–47], sensory cortex [48, 49], and posterior parietal cortex [50, 51]), with the most extensive studies on the PFC. In our previous study [36], we also found that 5XFAD mice had diminished neuronal activation in the mPFC when performing OWMC tasks. In the present study, we wanted to further clarify the activation of neurons in two subregions (the PrL and IL) of the mPFC when performing this task paradigm. Neuronal activation was attenuated in the PrL of 5XFAD mice but not in the IL. WM, as a cognitive process, requires the integration of transient sensory inputs over time and the maintenance of task-relevant stimulus representations [52]. Differences in attention, motivation, and motion can serve as confounding factors in WM assessments. If 5XFAD mice exhibit lower motivation, reduced reward responsiveness, and decreased activity, it could potentially lead to poorer task performance. Prior to training, we recorded the body weight and daily food intake of

the mice and found no differences between the 5XFAD and WT groups in these aspects [36]. Additionally, we implemented strict food restriction and provided a minimal amount of reward food pellets (0.05 g) to ensure the mice's motivation. At the end of each day's session, we provided food to the mice and observed that they consumed it quickly, indicating a strong motivation to eat even after the experiment. From the experimental results, it can be seen that there were no differences in performance between the 5XFAD and WT mice during the NMSS and NMMS training stages, further ruling out the possibility of differences in motivation, arousal, or reward processing between the two groups. Therefore, we propose that the attenuated activation of PrL neurons leads to the reduced WMC in the 5XFAD mice, rather than affecting their WMC through motivation, arousal, or reward processing. Previous evidence suggests that the PrL and IL regions can be functionally separated. In line with its connection to affective and autonomic structures, the IL appears to play a specific role in regulating fear-related behaviors, especially those related to eliminating emotional responses [53–55]. Compared to the functions of the IL, the PrL region is thought to be less involved in emotional aspects but more involved in cognitive functions, such as WM [35, 56–60]. Our findings are consistent with previous studies and provide further evidence of the importance of the PrL for WMC.

Different types of neurons in the mPFC play different roles in encoding and regulating behavior [61, 62]. The mPFC in rodents is primarily composed of a majority of excitatory glutamatergic pyramidal neurons and 15%-20% of inhibitory GABAergic interneurons. The function of the PFC relies on a delicate balance between excitation and inhibition, mediated by excitatory pyramidal neurons and various GABAergic interneurons [63, 64]. The majority (80%) of cortical interneurons are vasoactive intestinal polypeptide, parvalbumin, and somatostatin neurons [65]. These different types of interneurons are differentially regulated by sensory stimuli, motor behaviors, brain states, and neuromodulatory inputs [66, 67]. Therefore, different types of interneurons may play distinct roles in local computation and exert unique control over excitatory output [65, 68]. When assessing the cause to the cellular level, we found that the activation of PrL excitatory neurons was attenuated in 5XFAD mice performing the OWMC task. The immunohistochemistry results did not reveal any changes in inhibitory interneurons. We believe that this may be due to the relatively small proportion of inhibitory interneurons and their differentiation into multiple types, each with its own functions. As a result, immunohistochemistry may not effectively capture the activation of certain types or subsets of inhibitory interneurons.

Extracellular amyloid deposition in 5XFAD mice begins at approximately 2 months, first in layer V of the cortex and subiculum, and increases rapidly with age [41]. By 3 months of age, significant amyloid deposition was already present in the mPFC [36]. Soluble Aβ oligomers and amyloid plaques can alter the function of local neuronal circuits and large-scale networks by disrupting the balance of synaptic excitation and inhibition (E/I balance) in the brain [69]. Previous studies have found that the functional state of the PrL depends mainly on the coordinated activity of glutamatergic pyramidal neurons. This activity heavily depends on the cellular E/I dynamic balance [70, 71]. Furthermore, the imbalance of pyramidal neuron E/I is thought to contribute to many of the symptoms observed in neuropsychiatric disorders [71–73]. As early as 1995, Goldman-Rakic et al. proposed that WM depends on the ability of pyramidal neuron networks to fire continuously [74]. In addition, Tian et al. found that excitatory neurons in the PrL exhibited emergent properties in a context-dependent manner underlying a short-term memory-like behavior paradigm, which was not observed in 5XFAD mice [75]. From this, we can infer that the diminished activation of PrL excitatory neurons in 5XFAD mice during task performance is associated with reduced WMC. To strengthen this hypothesis, we used a chemogenetic method to modulate the inhibition and activation of excitatory neurons in WT and 5XFAD mice. As expected, inhibition of PrL excitatory neurons in WT mice reduced their WMC, and activation of PrL excitatory neurons in 5XFAD mice improved the impairment of their WMC. Therefore, we demonstrate that attenuated activation of PrL excitatory neurons in 5XFAD mice leads to a decrease in their WMC.

This study also has some limitations. We used 5XFAD mice to explore the neurobiological mechanisms of WM impairment in AD. We found that PrL excitatory neuron activation was diminished in 5XFAD mice. Is this phenomenon only present in 5XFAD mice, or is it also true in other AD models? We have yet to answer this question, which requires further studies. Previous behavioral research studies have predominantly been conducted on male mice. In order to establish a better comparative reference with these studies, only male mice were selected for our research. Therefore, we cannot be certain whether gender differences will have an impact on the results of our study. Moreover, in the present study, we did not detect neuronal electrical activity in the PrL brain region while the mice were performing the task, so we do not know the difference in neuronal firing activity between the two types of mice.

Conclusions

We found that diminished activation of excitatory neurons in the PrL led to impaired WMC in mice. These findings further extend to understanding the neurobiological mechanism of WM impairment in AD. Moreover, a possible intervention direction can be proposed: can WM impairment in AD be ameliorated by activating excitatory neuron firing? We need to explore this further.

Methods

Animals

5XFAD mice (overexpressing K670N/M671L + I716V + V717I mutations of human APP and M146L + L286V mutations of human PS1) were purchased from Jackson Laboratory (Bar Harbor, ME, USA, strain no. 008730). The WT littermates were used as controls. Age (3 months) and body weight were kept constant among experimental control factors. Mice were housed in a temperature- and humidity-controlled environment (22 ± 2 °C, 40–70%) with a 12-h light/12-h dark cycle. Prior to experiments, food and water were freely available. In this study, only male mice were used. All animal experimental procedures were conducted in accordance with the Guide for the Care and Use of Laboratory Animals (8th edition) and were approved by the Institutional Animal Care and Use Committee of Peking University.

OWMC task

The OWMC task involves five stages: context adaptation, digging training, NMSS rule-learning, NMMS rule-learning, and capacity testing (Fig. 6a). In the first stage, mice are handled to reduce stress and acclimate to the training cage (Fig. 6b). The second stage involves training mice to dig in a bowl of unscented sawdust to locate a piece of cheese (Fig. 6c). In the third stage, mice are trained to find cheese pellets in a bowl with a novel odor (Fig. 6d). The fourth stage requires mice to discern the novel odor among multiple scented bowls to find the cheese pellet (Fig. 6e). Finally, in the fifth stage, mice undergo several WMC tests until they achieve a stable level of performance (Fig. 6e). For further detail regarding this paradigm, please refer to our previously published article [37].

Tissue preparation

After 24 h of the capacity test, 5XFAD mice and littermates were randomly divided into 4 groups (5XFAD + OWMC task, WT + OWMC task, 5XFAD + non-OWMC task, WT + non-OWMC task). Mice in the task groups

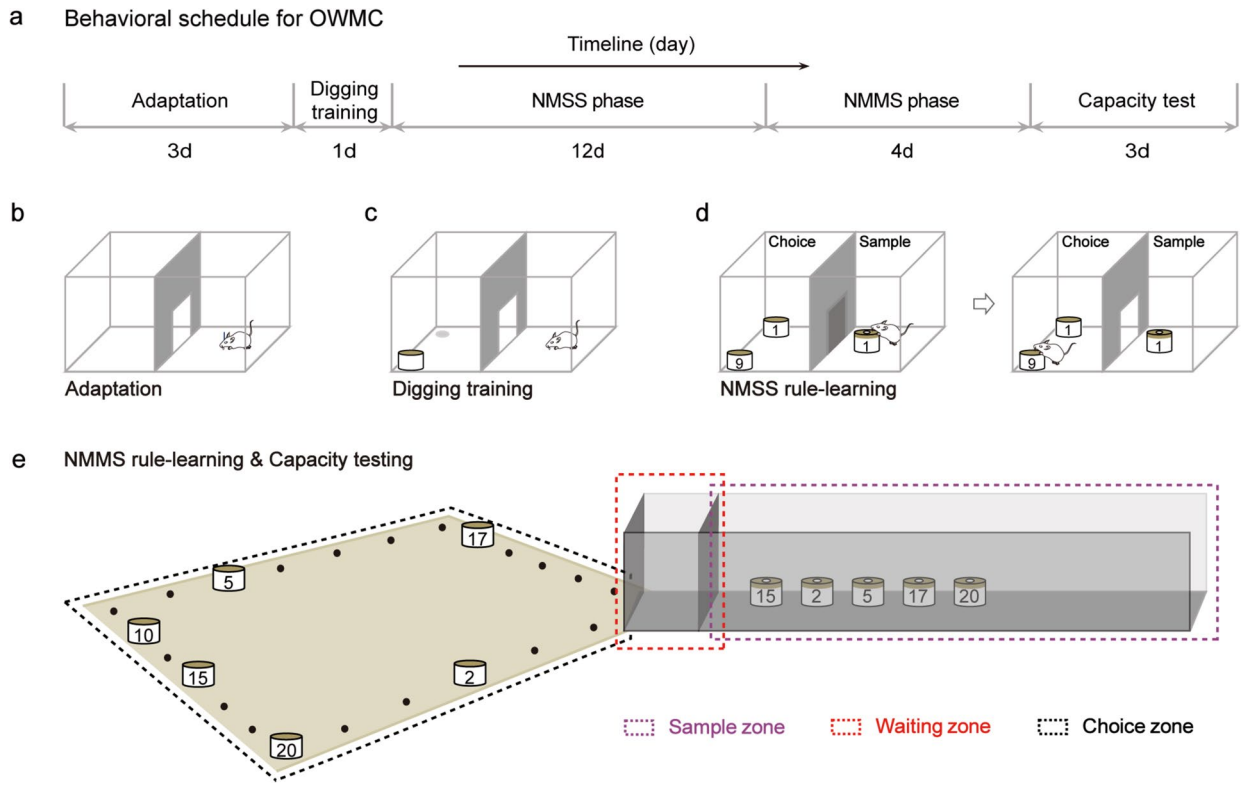

Fig. 6 Schematic diagram of the OWMC task. **a** Timeline of the OWMC task. **b** Context adaptation of the OWMC task. **c** Digging training phase of the OWMC task. **d** NMSS rule-learning phase of the OWMC task. **e** NMMS rule-learning and capacity testing phase of the OWMC task

performed 2 capacity test trials, a 3-sample and a 6-sample trial, while mice in the nontask groups entered a cage and freely detected the same odors as the task groups. Then, the mice in the nontask group entered the empty sample zone and received a piece of cheese in the empty selection zone. Ninety minutes after the behavioral assessments, mice were deeply anesthetized and perfused with 30 ml of 0.9% saline via the cardiac artery, followed by 30 ml of 4% paraformaldehyde (PFA). The brains were removed and immersed in 10 ml of 4% PFA at 4 °C for 24 h. The PFC region of the brains was sliced into 30-μm-thick sections from the coronal plane with a freezing microtome. Sections were collected for immunohistochemistry.

Immunohistochemistry and microscopy

Slices were washed 3 times with 0.1 M PBS for 5 min to remove the OCT. The slices were subsequently permeabilized and blocked in 0.1 M PBS containing 0.3% Triton X-100 and 5% bovine serum albumin (BSA) for 1 h at room temperature (RT). Next, slices were incubated overnight with the primary antibodies (anti-c-FOS, 1:1000, 2250 s, Cell Signaling Technology; anti-c-FOS, 1:1000, ab208942, Abcam; anti-CaMKII, 1:1000, ab52476, Abcam; anti-GAD65 + GAD67, 1:1000, ab183999, Abcam) diluted in blocking solution at 4 °C, and unbound antibody was removed by rinsing with 0.1 M PBS. Then, the brain slices were incubated in species-specific secondary antibodies (Alexa Fluor 488-conjugated goat anti-rabbit, 1:500, ab150077, Abcam; Alexa Fluor 594-conjugated goat anti-mouse, 1:500, ab150116, Abcam) diluted in 0.1 M PBS with 5% BSA for 1 h at RT. Finally, the slices were washed 3 times with 0.1 M PBS for 5 min each to remove excess secondary antibodies, and the nuclei were stained with DAPI (1:1000; Sigma Chemical) for 20 min at RT. Images were acquired using the Zeiss Axio Scan. Z1 Digital Slide Scanner. In this study, we utilized an aplan apochromat 20 × /0.8 M27 objective for imaging. The light source employed was HXP120V. The beam filters utilized were as follows: Filter 395 (Excitation: 330–375 nm; Emission: 430–470 nm), Filter 498 (Excitation: 453–485 nm; Emission: 507–546 nm), and Filter 603 (Excitation: 581–593 nm; Emission: 618–675 nm). The imaging device used was the Orca Flash 4.0. The acquired images have a bit depth of 16 bits, and we utilized Zen Blue 2 software to capture images of specific brain regions. Three slices from each mouse were selected for analysis. Furthermore, ImageJ was used to count and analyze the number of immunopositive cells. The scale bars are 50 μm, and each image area is 350 μm × 300 μm.

Virus injection

The mice were anesthetized with tribromoethanol (240 mg/kg, Sigma) and then fixed on a stereotaxic frame (RWD Life Science, Shenzhen, China). After horizontal adjustment of the skull position under a stereomicroscope (RWD Life Science, Shenzhen, China), a minor craniotomy was performed with a thin drill over the PrL (typical coordinate: 1.98 mm anterior to Bregma; 0.32 mm lateral to the midline). Adeno-associated virus (AAV) carrying the hM3D (AAV-CaMKIIα-hM3D(Gq)–mCherry) and hM4D (AAV-CaMKIIα-hM4D(Gi)-mCherry) fusion genes or mcherry (AAV-CaMKIIα -mcherry) was injected through a microsyringe pump at 40 nL/min using a 5 μL microsyringe (#700, Hamilton, USA). A total of 80 nL of the virus was injected at a depth of 2.05 mm from the Bregma. At the end of the infusion, the pipette was held for 10 min to allow the virus to spread. hM3Dq (TG: $n = 6$) was injected for activation, and hM4Di (WT: $n = 7$) was injected for inhibition by bilateral injection. Control experiments were conducted using adenovirus expressing only mCherry and bilaterally injected in both WT ($n = 5$) and TG ($n = 5$) subjects. The viruses hM3Dq ($AAV_{2/9}$, titer: 2.0×10^{12} v.g./mL) and hM4Di ($AAV_{2/9}$, titer: 2.0×10^{12} v.g./mL) or mCherry ($AAV_{2/9}$, titer: 2.0×10^{12} v.g./mL) were made by BrainVTA (Wuhan, China). Experiments were performed at least 4 weeks after virus injection. The mice that were injected with the above virus received a saline intraperitoneal injection (i.p.) to test the baseline WMC of the mice. Subsequently, to manipulate the neurons, CNO (1 mg/kg; A3317, APExBIO, USA) was administered to the mice via i.p. for viral infection.

Slice electrophysiology

After 4 weeks of viral incubation, coronal sections, including PrL, were cut at a thickness of 300 μm in ice-cold cutting solution (185 mM sucrose, 2.5 mM KCl, 1.25 mM $NaH_2PO_4 \cdot 2H_2O$, 25 mM $NaHCO_3$, 25 mM D-glucose, 0.5 mM $CaCl_2 \cdot 2H_2O$, 10 mM $MgSO_4$, oxygenated with 95% O2/5% CO_2) using a vibrating microtome (VT 1200S, Leica, Germany). Next, slices were incubated in aerated (95% O2/5% CO_2) artificial cerebrospinal fluid (ACSF: 125 mM NaCl, 2.5 mM KCl, 1.25 mM $NaH_2PO_4 \cdot 2H_2O$, 25 mM $NaHCO_3$, 10 mM D-glucose, 2 mM $CaCl_2 \cdot 2H_2O$, 1.5 mM $MgSO_4$, pH 7.4), recovered at 32 °C for 30 min, and subsequently incubated at RT for 30 min. The pipettes were connected to the headstage of the Heka EPC 10 amplifier (Heka Elektronik, USA). Cells expressing mCherry in the PrL were identified on a microscope equipped with a differential interference contrast optical system (BX51WI, Olympus, Japan). Current-clamp

recordings were applied to measure evoked action potentials in CNO activation and inhibition experiments. After applying current in 20 pA steps (from -60 to 300 pA), the neurons recovered for 5 min. Then, the slices were perfused with ACSF containing 5 μM CNO. The same procedure was performed 10 min after CNO perfusion.

Statistical analysis

All data are presented as the mean ± standard error of the mean (SEM), and statistical tests were performed using GraphPad Prism version 9.0 software. Two-way analysis of variance (ANOVA) was used to analyze the effects of memory capacity and mouse genotype (wild-type or 5XFAD), the effects of current and CNO intervention, or the effects of memory capacity and virus intervention. Two-way ANOVA was also performed to analyze the effects of task and mouse genotype, and post hoc Tukey's tests were applied to analyze the differences between groups. Linear regression was utilized to analyze the correlation between memory capacity and the number of FOS^+ neurons, as well as the correlation between the number of FOS^+ neurons and the number of FOS^+ neurons co-localized with $CaMKII^+$ neurons. We used Student's *t* tests to analyze the other data. The statistical significance threshold for all tests was set at $p < 0.05$.

Abbreviations

AD	Alzheimer's disease
WM	Working memory
WMC	Working memory capacity
PFC	Prefrontal cortex
mPFC	Medial prefrontal cortex
OWMC	Olfactory working memory capacity
PrL	Prelimbic cortex
IL	Infralimbic cortex
TG	5XFAD
WT	Wild-type
NMSS	Nonmatching to a single odor sample
NMMS	Nonmatching to multiple odor samples
FOS^+	FOS-positive
$CaMKII^+$	Calmodulin-dependent protein kinase II-positive
GAD^+	Glutamate decarboxylase-positive
CNO	Clozapine-N-oxide
E/I	Excitation and inhibition
PFA	Paraformaldehyde
BSA	Bovine serum albumin
RT	Room temperature

Supplementary Information

The online version contains supplementary material available at https://doi.org/10.1186/s12915-023-01674-3.

Additional file 1. Individual values for figures. Each sheet in the Excel file is named by the figure.

Acknowledgements

We thank the National Center for Protein Sciences at Peking University in Beijing, China, for assisting us with the image acquisition and stereotactic injection of viruses and Li-Qin Fu for helping us with the image optimization. We thank Wei-Min Dang from Peking University Institute of Mental Health (Sixth Hospital) for their help in the smooth conduct of the experiment.

Authors' contributions

L.X.J., G.D.H. and X.Y. designed the experiments. L.X.J., G.D.H., Y.L.T., R.X.C. and X.M. performed the experiments. L.X.J., G.D.H., Y.L.T., R.X.C. and X.M. analyzed and interpreted the data. L.X.J. and X.Y. wrote and reviewed the manuscript. H.L.W., C.Z., and X.Y. commented on the manuscript. All authors read and approved the final version.

Funding

This study was supported by grants from the National Key R&D Programme of China (Grant No. 2018YFC1314200), the National Natural Science Foundation of China (Grant No. 82101492) and the Shenzhen Science and Technology Program (Grant No. RCBS20221008093252091).

Availability of data and materials

All data generated or analyzed during this study are included in this published article and its supplementary information files. The individual data values are provided in Additional file 1.

Declarations

Ethics approval and consent to participate

All animal experimental procedures were approved by Institutional Animal Care and Use Committee of Peking University (No. Physics-ChenZZ-1).

Consent for publication

Not applicable.

Competing interests

The authors declare having no competing interests.

Author details

[1]Peking University Institute of Mental Health (Sixth Hospital), No.51 Huayuanbei Road, Haidian District, Beijing 100191, China. [2]National Clinical Research Center for Mental Disorders & NHC Key Laboratory of Mental Health (Peking University), Beijing 100191, China. [3]Beijing Municipal Key Laboratory for Translational Research On Diagnosis and Treatment of Dementia, Beijing 100191, China. [4]Department of Addiction Medicine, Shenzhen Clinical Research Center for Mental Disorders, Shenzhen Mental Health Center, Shenzhen Kangning Hospital, No.77 Zhenbi Road, Pingshan District, Shenzhen 518118, China. [5]Affiliated Mental Health Center, Southern University of Science and Technology, No.1088 Xueyuan Avenue, Fuguang Community, Taoyuan Street, Nanshan District, Shenzhen 518118, China. [6]School of Psychological and Cognitive Sciences, Peking University, No.5 Summer Palace Road, Haidian District, Beijing 100871, China. [7]IDG/McGovern Institute for Brain Research, Peking University, Beijing 100871, China. [8]Key Laboratory of Cell Proliferation and Differentiation of the Ministry of Education, College of Life Sciences, Peking University, Beijing 100871, China. [9]National Center of Gerontology, Beijing Hospital, No.1 Dahua Road, Dongdan, Dongcheng District, Beijing 100005, China. [10]Beijing Key Laboratory of Neural Regeneration and Repair, Advanced Innovation Center for Human Brain Protection, School of Basic Medical Sciences, Capital Medical University, No.10 Xitoutiao, You'anmenwai, Fengtai District, Beijing 100069, China.

Received: 9 February 2023 Accepted: 1 August 2023
Published online: 11 August 2023

References

1. Alzheimer's Disease International. World Alzheimer's Report 2015: The global impact of dementia. 2015.
2. Scheltens P, De Strooper B, Kivipelto M, Holstege H, Chételat G, Teunissen CE, et al. Alzheimer's disease. Lancet. 2021;397(10284):1577–90.
3. Long JM, Holtzman DM. Alzheimer disease: an update on pathobiology and treatment strategies. Cell. 2019;179(2):312–39.

4. Jack CR, Bennett DA, Blennow K, Carrillo MC, Dunn B, Haeberlein SB, et al. NIA-AA Research Framework: toward a biological definition of Alzheimer's disease. Alzheimer's Dement. 2018;14(4):535–62.
5. Karran E, De Strooper B. The amyloid hypothesis in Alzheimer disease: new insights from new therapeutics. Nat Rev Drug Discov. 2022;21(4):306–18.
6. Perry RJ, Watson P, Hodges JR. The nature and staging of attention dysfunction in early (minimal and mild) Alzheimer's disease: relationship to episodic and semantic memory impairment. Neuropsychologia. 2000;38(3):252–71.
7. Kaushik M, Kaushik P, Parvez S. Memory related molecular signatures: the pivots for memory consolidation and Alzheimer's related memory decline. Ageing Res Rev. 2022;76:1–11.
8. Bondi MW, Jak AJ, Delano-Wood L, Jacobson MW, Delis DC, Salmon DP. Neuropsychological contributions to the early identification of Alzheimer's disease. Neuropsychol Rev. 2008;18(1):73–90.
9. Storandt M, Grant EA, Miller JP, Morris JC. Longitudinal course and neuropathologic outcomes in original vs revised MCI and in pre-MCI. Neurology. 2006;67(3):467–73.
10. Twamley EW, Ropacki SA, Bondi MW. Neuropsychological and neuroimaging changes in preclinical Alzheimer's disease. J Int Neuropsychol Soc. 2006;12(5):707–35.
11. Webster SJ, Bachstetter AD, Nelson PT, Schmitt FA, Van Eldik LJ. Using mice to model Alzheimer's dementia: an overview of the clinical disease and the preclinical behavioral changes in 10 mouse models. Front Genet. 2014;5:1–23.
12. Saunders NLJ, Summers MJ. Longitudinal deficits to attention, executive, and working memory in subtypes of mild cognitive impairment. Neuropsychology. 2011;25(2):237–48.
13. Kirova AM, Bays RB, Lagalwar S. Working memory and executive function decline across normal aging, mild cognitive impairment, and Alzheimer's Disease. Biomed Res Int. 2015;2015:1–9.
14. Grady C. The cognitive neuroscience of ageing. Nat Rev Neurosci. 2012;13(7):491–505.
15. Park DC, Reuter-Lorenz P. The adaptive brain: aging and neurocognitive scaffolding. Annu Rev Psychol. 2009;60:173–96.
16. Belleville S, Chertkow H, Gauthier S. Working Memory and Control of Attention in Persons With Alzheimer's Disease and Mild Cognitive Impairment. Neuropsychology. 2007;21(4):458–69.
17. Huntley JD, Howard RJ. Working memory in early Alzheimer's disease: a neuropsychological review. Int J Geriatr Psychiatry. 2010;25(2):121–32.
18. Stopford CL, Thompson JC, Neary D, Richardson AMT, Snowden JS. Working memory, attention, and executive function in Alzheimer's disease and frontotemporal dementia. Cortex. 2012;48(4):429–46.
19. Constantinidis C, Klingberg T. The neuroscience of working memory capacity and training. Nat Rev Neurosci. 2016;17(7):438–49.
20. Miller EK, Lundqvist M, Bastos AM. Working Memory 2.0. Neuron. 2018;100(2):463–75.
21. Lundqvist M, Herman P, Miller EK. Working memory: delay activity, yes! persistent activity? Maybe not. J Neurosci. 2018;38(32):7013–9.
22. Hasselmo ME, Stern CE. Mechanisms underlying working memory for novel information. Trends Cogn Sci. 2006;10(11):487–93.
23. Ma WJ, Husain M, Bays PM. Changing concepts of working memory. Nat Neurosci. 2014;17(3):347–56.
24. Luck SJ, Vogel EK. Visual working memory capacity: from psychophysics and neurobiology to individual differences. Trends Cogn Sci. 2013;17(8):391–400.
25. Cowan N. The magical number 4 in short-term memory: a reconsideration of mental storage capacity. Behav Brain Sci. 2001;24(1):87–114.
26. Bastos AM, Loonis R, Kornblith S, Lundqvist M, Miller EK. Laminar recordings in frontal cortex suggest distinct layers for maintenance and control of working memory. Proc Natl Acad Sci U S A. 2018;115(5):1117–22.
27. Lara AH, Wallis JD. The role of prefrontal cortex in working memory: A mini review. Front Syst Neurosci. 2015;9(DEC):1–7.
28. Yan Z, Rein B. Mechanisms of synaptic transmission dysregulation in the prefrontal cortex: pathophysiological implications. Mol Psychiatry. 2022;27(1):445–65.
29. Baeg EH, Kim YB, Huh K, Mook-Jung I, Kim HT, Jung MW. Dynamics of population code for working memory in the prefrontal cortex. Neuron. 2003;40(1):177–88.
30. Romo R, Brody CD, Hernández A, Lemus L. Neuronal correlates of parametric working memory in the prefrontal cortex. Nature. 1999;399(6735):470–3.
31. Fujisawa S, Amarasingham A, Harrison MT, Buzsáki G. Behavior-dependent short-term assembly dynamics in the medial prefrontal cortex. Nat Neurosci. 2008;11(7):823–33.
32. Erlich JC, Bialek M, Brody CD. A cortical substrate for memory-guided orienting in the rat. Neuron. 2011;72(2):330–43.
33. Meyers EM, Qi XL, Constantinidis C. Incorporation of new information into prefrontal cortical activity after learning working memory tasks. Proc Natl Acad Sci U S A. 2012;109(12):4651–6.
34. Liu D, Gu X, Zhu J, Zhang X, Han Z, Yan W, et al. Medial prefrontal activity during delay period contributes to learning of a working memory task. Science. 2014;346(6208):458–63.
35. Vogel P, Hahn J, Duvarci S, Sigurdsson T. Prefrontal pyramidal neurons are critical for all phases of working memory. Cell Rep. 2022;39(2):1–15.
36. Huang G-D, Jiang L-X, Su F, Wang H-L, Zhang C, Yu X. A novel paradigm for assessing olfactory working memory capacity in mice. Transl Psychiatry. 2020;10(1):1–16.
37. Jiang LX, Di HG, Wang HL, Zhang C, Yu X. The protocol for assessing olfactory working memory capacity in mice. Brain Behav. 2022;12(8):1–10.
38. Dudchenko PA, Wood ER, Eichenbaum H. Neurotoxic hippocampal lesions have no effect on odor span and little effect on odor recognition memory but produce significant impairments on spatial span, recognition, and alternation. J Neurosci. 2000;20(8):2964–77.
39. Young JW, Kerr LE, Kelly JS, Marston HM, Spratt C, Finlayson K, et al. The odour span task: a novel paradigm for assessing working memory in mice. Neuropharmacology. 2007;52(2):634–45.
40. Bhattacherjee A, Djekidel MN, Chen R, Chen W, Tuesta LM, Zhang Y. Cell type-specific transcriptional programs in mouse prefrontal cortex during adolescence and addiction. Nat Commun. 2019;10(1):1–18.
41. Oakley H, Cole SL, Logan S, Maus E, Shao P, Craft J, et al. Intraneuronal β-amyloid aggregates, neurodegeneration, and neuron loss in transgenic mice with five familial Alzheimer's disease mutations: potential factors in amyloid plaque formation. J Neurosci. 2006;26(40):10129–40.
42. Kimura R, Ohno M. Impairments in remote memory stabilization precede hippocampal synaptic and cognitive failures in 5XFAD Alzheimer mouse model. Neurobiol Dis. 2009;33(2):229–35.
43. Devi L, Ohno M. Phospho-eIF2α level is important for determining abilities of BACE1 reduction to rescue cholinergic neurodegeneration and memory defects in 5XFAD mice. PLoS ONE. 2010;5(9):1–10.
44. Lin Y, Jin J, Lv R, Luo Y, Dai W, Li W, et al. Repetitive transcranial magnetic stimulation increases the brain's drainage efficiency in a mouse model of Alzheimer's disease. Acta Neuropathol Commun. 2021;9(1):1–18.
45. Kane MJ, Engle RW. The role of prefrontal cortex in working-memory capacity, executive attention, and general fluid intelligence: an individual-differences perspective. Psychon Bull Rev. 2002;9(4):637–71.
46. Minamoto T, Yaoi K, Osaka M, Osaka N. The rostral prefrontal cortex underlies individual differences in working memory capacity: an approach from the hierarchical model of the cognitive control. Cortex. 2015;71:277–90.
47. Yoon JH, Grandelis A, Maddock RJ. Dorsolateral prefrontal cortex GABA concentration in humans predicts working memory load processing capacity. J Neurosci. 2016;36(46):11788–94.
48. D'Esposito M, Postle BR. The cognitive neuroscience of working memory. Annu Rev Psychol. 2015;66:115–42.
49. Ku Y, Bodner M, Di ZY. Prefrontal cortex and sensory cortices during working memory: quantity and quality. Neurosci Bull. 2015;31(2):175–82.
50. Vogel EK, Machizawa MG. Neural activity predicts individual differences in visual working memory capacity. Nature. 2004;428(6984):748–51.
51. Todd JJ, Marois R. Capacity limit of visual short-term memory in human posterior parietal cortex. Nature. 2004;428(6984):751–4.
52. Curtis CE, Lee D. Beyond working memory: the role of persistent activity in decision making. Trends Cogn Sci. 2010;14(5):216–22.
53. Soler-cedeño O, Cruz E, Criado-marrero M, Porter JT. Contextual fear conditioning depresses infralimbic excitability. Neurobiol Learn Mem. 2016;130:77–82.
54. Santini E, Quirk GJ, Porter JT. Fear conditioning and extinction differentially modify the intrinsic excitability of infralimbic neurons. J Neurosci. 2008;28(15):4028–36.

55. Izquierdo A, Wellman CL, Holmes A. Brief uncontrollable stress causes dendritic retraction in infralimbic cortex and resistance to fear extinction in mice. J Neurosci. 2006;26(21):5733–8.
56. Chudasama Y, Robbins TW. Dopaminergic modulation of visual attention and working memory in the rodent prefrontal cortex. Neuropsychopharmacology. 2004;29(9):1628–36.
57. Touzani K, Puthanveettil SV, Kandel ER. Consolidation of learning strategies during spatial working memory task requires protein synthesis in the prefrontal cortex. Proc Natl Acad Sci U S A. 2007;104(13):5632–7.
58. Gimenez G, Van WC, Darbanfouladi M. A cell type – specific cortico-subcortical brain circuit for investigatory and novelty-seeking behavior. Science. 2021;372(6543):1–9.
59. Maksymetz J, Byun NE, Luessen DJ, Li B, Barry RL, Gore JC, et al. mGlu1 potentiation enhances prelimbic somatostatin interneuron activity to rescue schizophrenia-like physiological and cognitive deficits. Cell Rep. 2021;37(5):1-14.e6.
60. Anderson EM, Loke S, Wrucke B, Engelhardt A, Demis S, O'Reilly K, et al. Suppression of pyramidal neuron G protein-gated inwardly rectifying K+ channel signaling impairs prelimbic cortical function and underlies stress-induced deficits in cognitive flexibility in male, but not female, mice. Neuropsychopharmacology. 2021;46(12):2158–69.
61. Xu H, Liu L, Tian Y, Wang J, Li J, Zheng J, et al. A Disinhibitory microcircuit mediates conditioned social fear in the prefrontal cortex. Neuron. 2019;102(3):668-682.e5.
62. Zhang C, Zhu H, Ni Z, Xin Q, Zhou T, Wu R, et al. Dynamics of a disinhibitory prefrontal microcircuit in controlling social competition. Neuron. 2022;110:1–16.
63. Kamigaki T, Dan Y. Delay activity of specific prefrontal interneuron subtypes modulates memory-guided behavior. Nat Neurosci. 2017;20(6):854–63.
64. Kvitsiani D, Ranade S, Hangya B, Taniguchi H, Huang JZ, Kepecs A. Distinct behavioural and network correlates of two interneuron types in prefrontal cortex. Nature. 2013;498(7454):363–6.
65. Kepecs A, Fishell G. Interneuron cell types are fit to function. Nature. 2014;505(7483):318–26.
66. Hattori R, Kuchibhotla KV, Froemke RC, Komiyama T. Functions and dysfunctions of neocortical inhibitory neuron subtypes. Nat Neurosci. 2017;20(9):1199–208.
67. Zhang S, Xu M, Kamigaki T, Do JPH, Chang WC, Jenvay S, et al. Long-range and local circuits for top-down modulation of visual cortex processing. Science. 2014;345(6197):660–5.
68. Huang ZJ. Toward a genetic dissection of cortical circuits in the mouse. Neuron. 2014;83(6):1284–302.
69. Busche MA, Konnerth A. Impairments of neural circuit function in Alzheimer's disease. Philos Trans R Soc B Biol Sci. 2016;371(1700):1–10.
70. Isaacson JS, Scanziani M. How inhibition shapes cortical activity. Neuron. 2011;72(2):231–43.
71. Yizhar O, Fenno LE, Prigge M, Schneider F, Davidson TJ, Ogshea DJ, et al. Neocortical excitation/inhibition balance in information processing and social dysfunction. Nature. 2011;477(7363):171–8.
72. Gonzalez-Burgos G, Lewis DA. NMDA receptor hypofunction, parvalbumin-positive neurons, and cortical gamma oscillations in schizophrenia. Schizophr Bull. 2012;38(5):950–7.
73. Covington HE, Lobo MK, Maze I, Vialou V, Hyman JM, Zaman S, et al. Antidepressant effect of optogenetic stimulation of the medial prefrontal cortex. J Neurosci. 2010;30(48):16082–90.
74. Goldman-Rakic PS. Cellular basis of working memory. Neuron. 1995;14(3):477–85.
75. Tian Y, Yang C, Cui Y, Su F, Wang Y, Wang Y, et al. An excitatory neural assembly encodes short-term memory in the prefrontal cortex. Cell Rep. 2018;22(7):1734–44.

Publisher's Note